A Study of Cooperative Phenyl Ring Flip Motions in Glassy Polystyrene by Molecular Simulations

Rajesh Khare and Michael E. Paulaitis*

Center for Molecular and Engineering Thermodynamics, Department of Chemical Engineering, University of Delaware, Newark, Delaware 19716

Received December 21, 1994; Revised Manuscript Received March 13, 1995[⊗]

ABSTRACT: Phenyl ring flip motion in polystyrene involves a cooperative movement of the phenyl ring and the chain backbone. In previous work, we described this cooperative rotation in single chains of polystyrene by defining the conformational transition in terms of a multidimensional reaction path and calculating torsion angle and energy profiles along this path. In this paper, we have extended our approach to study phenyl ring rotation in model structures of atactic polystyrene glasses. Reaction paths, energy profiles, free energy barriers, and rate constants were calculated for the rotation of 10 different phenyl rings in the same local backbone conformation. The results show that local intrachain steric interactions, that dominate rotation in single chains, do so in the polymer glass as well. In addition, the free energy barriers cover a wide range of values corresponding to a distribution of characteristic times for ring rotation that spans 21 decades. This distribution is also bimodal. The results are compared with observations from NMR experiments and previous molecular mechanics calculations.

Introduction

Macroscopic mechanical and transport properties of polymers are influenced by local chain motions or conformational transitions that are manifested in various relaxation processes. Knowledge of the molecular mechanisms and the kinetics of such transitions is important, not only from the perspective of understanding fundamental structure–property relationships but also in practice, for the rational design of polymeric materials with specific properties. Since it is not always possible to obtain from experiments unequivocal information about molecular mechanisms underlying such motions, complementary approaches to evaluating conceivable mechanisms are desirable. Molecular simulations provide one such approach. In recent years, a number of computational studies have focused on the short-time (approximately picoseconds to nanoseconds) dynamics of polymer chains. Specific studies include Brownian dynamics investigations of the mechanisms of backbone conformational transitions for polyethylene[1,2] and for polyisoprene in solution;[3] molecular dynamics investigations of polyethylene in the bulk;[4,5] and molecular dynamics simulations of short-time (approximately picoseconds) chain motions for single chains of polyimide and polystyrene, and glassy polystyrene.[6] Conformational transitions that take place on longer time scales cannot be studied using these techniques; hence, new simulation methodologies must be developed. One such conformational transition is phenyl ring rotation in polystyrene glasses. Recent reviews of experimental observations of this transition can be found elsewhere.[7,8] We present a brief summary below.

Conformational mobility attributed to local chain motions in polystyrene (hereafter abbreviated PS) is revealed in various subglass relaxation processes observed in dynamic mechanical,[9–11] dielectric,[11,12] and NMR spin–lattice relaxation experiments.[13] There is general agreement from this body of work that PS exhibits at least three subglass relaxations. The local chain motion related to the γ relaxation is hypothesized to be a cooperative conformational transition that includes phenyl ring flips of 180° coupled with small-amplitude motions by the main chain. This relaxation is observed over a range of temperatures near 180 K, occurs at a frequency of approximately 10 kHz at this temperature, and has an activation energy of approximately 9 kcal/mol.[11]

Spiess[14,15] examined the 180° ring flip transition in deuterated atactic PS glasses using ^{2}H NMR spectroscopy and concluded that approximately 20% of the phenyl rings exhibit rapid 180° flips about the ring axis defined by the carbon bond connecting the phenyl ring to the backbone of the polymer chain. The rotational correlation time for this motion was estimated to be 10^{-7}–10^{-8} s, indicating that ring flips occur infrequently compared to small-amplitude (±15°) oscillations about the ring axis which have correlation times on the order of 10^{-13} s.

Schaefer and co-workers[16,17] studied phenyl ring rotation in PS glasses using ^{13}C NMR spectroscopy and interpreted their observations in terms of a concerted motion consisting of 180° flips coupled with restricted main-chain reorientations. The rotational correlation time was found to be on the order of 10^{-7} s, which is consistent with the observation of the γ transition at 153 K and a frequency of 1 Hz, when this frequency is extrapolated to room temperature using the measured activation energy of 10 kcal/mol. Since only 7% of the phenyl rings were found to execute 180° ring flips, it was speculated that the cooperative motion can only occur in those regions of the glass where chain packing results in high main-chain flexibility. Experiments carried out on various substituted polystyrenes supported this hypothesis.

Previous molecular mechanics calculations of ring flip motion in single chains of PS aimed at reproducing the experimental value of the activation energy for the γ relaxation. Tonelli[18] reported energy barriers for ring flips that were greater than 100 kcal/mol, implying that there are large steric barriers to ring rotation. Backbone dihedral angles in these calculations were, however, constrained to their initial values as the torsional angle for ring rotation was driven through 180°. Hägele and Beck[19] improved upon these calculations by allowing the backbone dihedral angles to relax as the ring was rotated. Significantly lower energy barriers of 10–20 kcal/mol were obtained which suggested that some

[⊗] Abstract published in *Advance ACS Abstracts,* May 15, 1995.

0024-9297/95/2228-4495$09.00/0

degree of cooperative motion is required between the phenyl ring and the chain backbone. However, it was not clear whether these two results differed because cooperative motion must be considered or because different sets of parameters were used to describe the nonbonded interactions in the two calculations. Recognizing this, Tanabe[20] accounted for the cooperative motion in an empirical fashion by forcing the two backbone dihedral angles adjacent to the phenyl ring to rotate in equal but opposite directions as the ring was rotated. Energy barriers of 10–50 kcal/mol were obtained with the potential energy parameters from the original work of Tonelli.[18] Although these energy barriers are, on average, significantly higher than the experimental value for the activation energy of the γ relaxation, they are much less than those obtained by Tonelli and therefore clearly show the cooperative nature of the transition.

In contrast to the number of atomistic simulation studies reported in the literature on conformational transitions in single chains of PS and other polymers, studies of conformational transitions in polymer glasses are scarce. As noted previously,[7,8,21,22] transitions such as phenyl ring rotation in polystyrene cannot be captured in conventional dynamics simulations since they occur on much slower time scales ($\sim 10^{-7}$ s) compared to that of a typical simulation run ($\sim 10^{-9}$ s). An alternative approach is to define a reaction coordinate for the conformational transition of interest and then use transition state theory[23–27] to calculate the rate at which this transition takes place. The approach has been applied to calculate the rate of aromatic ring rotation for tyrosine-35 in the protein, bovine pancreatic trypsin inhibitior,[28] and the rate of concerted ring rotation in the active site of tosyl-α-chymotrypsin.[29] Conformational transitions in synthetic polymer glasses have also been studied. Smith and Boyd[22] calculated free energy barriers for rotation of a methyl acrylate-type ester side group incorporated in the chain of bulk polyethylene. In their implementation, free energies were obtained from molecular dynamics simulations by applying umbrella sampling along the reaction coordinate. Suter and co-workers studied phenyl ring flips and other local motions in PS[7] and polycarbonate[21] glasses. For ring rotation in PS, the reaction coordinate was defined to be the single dihedral angle for rotation around the ring axis. Energy profiles along this reaction coordinate were obtained from molecular mechanics by rotating this dihedral angle through 180° in increments of 5° while minimizing the energy at each step with respect to all other degrees of freedom. The free energy barrier for the transition was assumed to be equal to the energy barrier; *i.e.*, the entropy of the transition was neglected. A broad distribution of energy barriers from 0.23 to 266.5 kcal/mol was obtained with a mean value of 27.7 kcal/mol. A typical energy profile exhibits a number of intermediate maxima and discontinuities of approximately 25 kcal/mol in magnitude (see, for example, Figure 12 in ref 7). Based on their observations, a "cogwheel and ratchet" mechanism for the ring flip transition was proposed in which the rotation takes places in a series of short, sudden steps. The influence of ring rotation was also observed to be far-reaching; *i.e.*, perturbations in the glass structure were seen over the entire length scale of the simulation box.

Molecular mechanics studies of phenyl ring flip motion in single chains of PS indicate that the transition takes place through a cooperative movement of the phenyl ring and the chain backbone. We recently reported results on this cooperative motion in single chains by defining a multidimensional reaction coordinate in the context of transition state theory.[8] Reaction paths and energy profiles along these paths were presented for three different chain conformations for both syndiotactic and isotactic hexamers. In this work, we have extended our investigations to ring rotation in model structures of PS glasses.[30] We begin by giving a brief description of our internal coordinate approach for locating transition states and reaction paths of conformational transitions. Next, results are presented for the rotation of 10 different phenyl rings having the same local chain conformation in our model PS glass structures. These results are compared with observations from NMR experiments and previous molecular mechanics studies. Finally, we discuss the nature of the cooperative motion between the rotating phenyl ring and the chain backbone and present conclusions regarding the utility of our approach for describing these motions.

Methodology

The application of transition state (TS) theory requires determination of the reaction coordinate for the conformational transition of interest. The intrinsic reaction coordinate (IRC) or reaction path is defined as the steepest descent (SD) path from the TS, or saddle point, to local minima on the potential energy surface in the space of mass-weighted Cartesian coordinates.[31] The IRC represents the most probable path followed during the conformational transition and describes all the structural changes that take place. Several methods for determining the IRC have been devised. One approach is to calculate the optimal path between two local energy minima by applying energy minimization,[32–34] Monte Carlo,[35] or variational[36] methods. An alternative approach is to first determine the TS, usually by second derivative methods,[37] and then follow the gradient "downhill" in potential energy to the stable conformational states. In all previous applications of these methods, molecular conformations have been defined in terms of the Cartesian coordinates of the atoms in the system. Cartesian coordinate space has the advantages of generality and simplicity due to the Euclidean character of this coordinate space. However, the large dimensionality of the system is a major drawback, particularly in TS determinations where diagonalization of the Hessian of the potential energy is required.

Lazaridis *et al.*[38] proposed an alternative method for locating transition states and determining reaction paths of conformational transitions that employs an adiabatic projection of the potential energy surface in the space of "essential" internal coordinates of the system. Using a typical empirical function for the configurational energy of chain molecules, $E(\mathbf{b},\theta,\phi)$, where the internal coordinates are the bond lengths, $\mathbf{b} = (b_1, b_2, ..., b_{N-1})$, bond angles, $\theta = (\theta_1, \theta_2, ..., \theta_{N-2})$, and torsion angles, $\phi = (\phi_1, \phi_2, ..., \phi_{N-3})$, it was shown[38] that, to a good approximation, the Hessian, formed by the second derivatives of the energy with respect to the internal coordinates, assumes the block diagonal form:

$$\mathbf{H} = \begin{bmatrix} \mathbf{H}_{BB} & & \sim 0 \\ & \mathbf{H}_{\theta\theta} & \\ \sim 0 & & \mathbf{H}_{\phi\phi} \end{bmatrix} \tag{1}$$

In block diagonal form, the eigenvalues of the Hessian

will simply be the eigenvalues of the component matrices $\mathbf{H}_{BB}$, $\mathbf{H}_{\theta\theta}$, and $\mathbf{H}_{\phi\phi}$. Since $\mathbf{H}_{BB}$ and $\mathbf{H}_{\theta\theta}$ will also be diagonal,[38] their eigenvalues will be the diagonal elements themselves, which are large and positive. Therefore, if the Hessian has one and only one negative eigenvalue, corresponding to a first-order saddle point, this eigenvalue must be located in $\mathbf{H}_{\phi\phi}$. We concentrate, therefore, on the elements of $\mathbf{H}_{\phi\phi}$ to locate transition states.

In our implementation, energy minimizations with respect to bond lengths and bond angles are carried out to generate the adiabatic potential energy surface,

$$E_a(\phi) = E[\phi,\mathbf{b}_a(\phi),\theta_a(\phi)] \tag{2}$$

where the subscript denotes adiabatic values. The derivative of the adiabatic energy with respect to ϕ_i gives

$$\frac{\partial E_a}{\partial \phi_i} = \frac{\partial E}{\partial \phi_i} + \sum_j \left(\frac{\partial E}{\partial b_j}\right)\left(\frac{\partial b_j}{\partial \phi_i}\right) + \sum_j \left(\frac{\partial E}{\partial \phi_j}\right)\left(\frac{\partial \phi_j}{\partial \phi_i}\right) \tag{3}$$

where derivatives with respect to b_i and θ_i are taken holding all other internal coordinates constant and derivatives with respect to ϕ_i are taken holding all other torsional angles constant. (The subscripts on b_i and θ_i denoting adiabatic values have been omitted for clarity.) Since, by definition,

$$\frac{\partial E}{\partial b_j} = \frac{\partial E}{\partial \theta_j} = 0 \qquad \text{for all } j \tag{4}$$

on the adiabatic surface, then

$$\frac{\partial E_a}{\partial \phi_i} = \frac{\partial E}{\partial \phi_i} \tag{5}$$

on the adiabatic surface. Thus, gradients of the energy with respect to the torsion angles on the adiabatic energy surface are equivalent to these gradients on the full energy surface. The second derivatives of the adiabatic energy with respect to the ϕ_i give the diagonal elements of $\mathbf{H}_{\phi\phi}$,

$$\frac{\partial^2 E_a}{\partial \phi_i^{\,2}} = \frac{\partial^2 E}{\partial \phi_i^{\,2}} + \sum_j \sum_k \left(\frac{\partial^2 E}{\partial q_j\, \partial q_k}\right)\left(\frac{\partial q_j}{\partial \phi_i}\right)\left(\frac{\partial q_k}{\partial \phi_i}\right) \tag{6}$$

where q_j and q_k denote all bond lengths and bond angles. If the bond lengths and bond angles are indeed "stiff" degrees of freedom, the derivatives of q_j and q_k with respect to ϕ_i can be neglected, and

$$\frac{\partial^2 E_a}{\partial \phi_i^{\,2}} = \frac{\partial^2 E}{\partial \phi_i^{\,2}} \tag{7}$$

The same result is obtained for the second cross derivatives of E_a with respect to ϕ_i and ϕ_j. The coordinates q_j and q_k in eq 6 also include "nonessential" torsion angles that are mapped out of $\mathbf{H}_{\phi\phi}$ in the adiabatic approximation. However, unlike bond lengths and bond angles, these angles may change significantly along the reaction path. Equation 7 would hold, nonetheless, in the limit of weak coupling between the essential and nonessential torsion angles. Therefore, if any nonessential torsion angle is coupled to the essential mapping coordinates, as determined by eq 6, it must be redefined as an essential mapping coordinate, such that

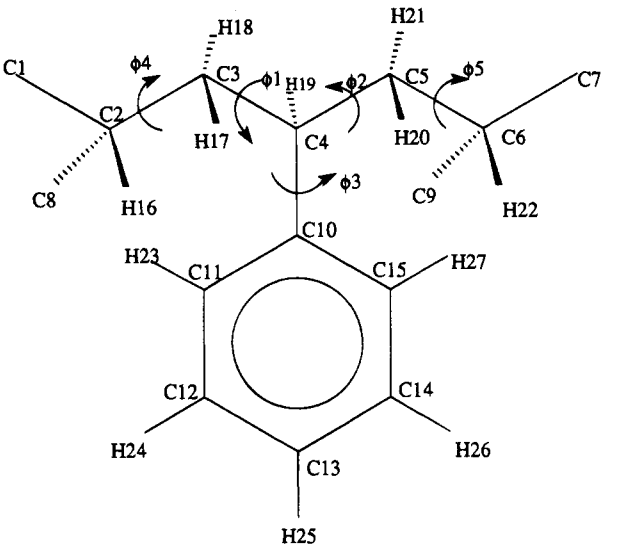

Figure 1. Section of a polystyrene chain showing two adjacent racemic diads. (Atoms C8 and C9 belong to neighboring phenyl rings which are not shown.)

$$\mathbf{H}_{\phi\phi} = \mathbf{H}_{\phi\phi,\text{adiab}} \tag{8}$$

The important implication of this analysis is that saddle points on the full potential energy surface will project onto saddle points on the adiabatic surface when energy minimizations are performed with respect to the stiff degrees of freedom, *i.e.*, the bond lengths and bond angles. Conversely, saddle points on the adiabatic energy surface correspond to transition states on the full energy surface. Therefore, the adiabatic projection retains all information needed to identify both the transition states and reaction coordinates of the conformational transition of interest.

The ring flip transition in PS is defined as a 180° rotation of the phenyl ring about the carbon–carbon bond connecting the ring to the backbone of the polymer chain, *i.e.*, the rotation of ϕ_3 in Figure 1. The important interactions governing this transition in single chains of PS are the steric interactions between the *ortho* hydrogens on the ring (H23, H27) and hydrogens on the first (H17, H18, H20, H21) and second (H16, H22) nearest-neighbor carbon atoms along the chain backbone.[8] The positions of these hydrogens relative to the ring are governed by the two backbone dihedral angles on either side of carbon atom C4, *i.e.*, the sequence of four backbone dihedral angles: ϕ_4, ϕ_1, ϕ_2, ϕ_5. However, rotations of the adjacent backbone torsion angles, ϕ_1 and ϕ_2, are more effective in relieving these steric interactions than rotations of ϕ_4 and ϕ_5. Therefore, our initial choice of "essential" mapping coordinates in the reaction path determinations will be the set of dihedral angles ϕ_1, ϕ_2, and ϕ_3. All other nonessential internal coordinates (bond lengths, bond angles, and nonessential dihedral angles) are mapped out in the adiabatic approximation.

Transition states on the $\phi_1\phi_2\phi_3$ adiabatic potential energy surface are located using the Cerjan–Miller algorithm.[37] The Hessian of the adiabatic energy was obtained numerically by calculating the change in energy for small changes (~4°) in the three essential dihedral angles, while minimizing the energy with respect to all other internal coordinates. The reproducibility of the adiabatic energy during these calculations was typically on the order of 0.01–0.1 kcal/mol. A starting TS conformation in the Cerjan–Miller algo-

Table 1. Structural Data for the Phenyl Rings Investigated

case no.	PS glass structure (number)	position of ring monomer in the PS 40-mer	angle between plane of phenyl ring and plane formed by the adjacent backbone bonds[a] (deg)			important interactions in the TS and their separations (in Å)
			TS	M1	M2	
I	1	9	48	92	92	H23–H16 (1.85), H27–H22 (2.01), H27–H20 (2.05)
II	3	19	40	87	78	H23–H16 (1.81), H27–H22 (1.82)
III	3	35	52	64	68	H23–H16 (1.79), H27–H22 (2.01)
IV	3	36	43	57	64	H23–H16 (1.95), H27–H22 (1.82), H27–*para*-H of ring 7 (2.04)
V	4	27	51	105	83	H23–H16 (1.82), H27–H22 (2.06)
VI	6	6	45	81	95	H23–H16 (1.88), H27–H22 (1.79), H23–*ortho*-H of ring 5 (1.97)
VII	6	21	48	82	99	H23–H16 (1.80), H27–H20 (2.10), H25–*para*-H of ring 30 (2.09)
VIII	8	18	50	104	78	H23–H16 (1.89), H27–H22 (1.77)
IX	10	12	44	73	66	H23–H16 (1.85), H27–H22 (1.84)
X	10	29	50	83	75	H23–H16 (1.87), H27–H22 (1.86) H24–backbone H on monomer 11 (1.97)

[a] TS denotes the transition state configuration, and M1 and M2 denote minimum-energy configurations.

rithm was generated by rotating primarily ϕ_3 such that the interactions between *ortho* hydrogens on the ring and hydrogens on backbone carbon atoms were strongly repulsive. In this configuration, the plane of the phenyl ring is roughly parallel to the axis of the chain backbone. A search starting from this conformation occasionally followed a trajectory in which one of the backbone dihedral angles changed from *trans* to *gauche*. In such cases, another starting TS conformation was generated by setting ϕ_1, ϕ_2, and ϕ_3 to their values for the TS conformation in the single chain.

Typically 30 iterations of the Cerjan–Miller algorithm were necessary to locate a TS. However, in two cases, the Cerjan–Miller algorithm failed to locate a TS when starting in either configuration. In these cases, the first-derivative method of Elber and co-workers[33,34] was used to locate an approximate TS conformation, which was then refined using either the Cerjan–Miller algorithm or finer grid points in the first-derivative algorithm. Once a TS was located, the IRC was calculated as the SD path on the adiabatic potential energy surface.[8,38] Computational details for locating the TS and IRC in each of the 10 cases studied are given elsewhere.[39]

The actual path followed during a ring flip process will oscillate about the IRC due to thermal fluctuations in the system. These fluctuations give rise to entropic contributions that depend on the local topology of the potential energy surface—*i.e.*, the "width of the valley" along the IRC—and require calculating the free energy profile along the IRC to obtain the probability of finding the system at the transition state at a finite temperature. The free energy profile can be evaluated by applying, for example, umbrella sampling[22] or free energy perturbation.[29] However, these techniques require inordinate amounts of computer time for the macromolecular systems of interest here. We have chosen instead to estimate the entropic contributions by applying a quadratic approximation for the potential energy surface near the TS and the local energy minima. In this approach, the potential energy profile is assumed to be sufficiently steep such that contributions to the entropy along the IRC are dominated by the topology of the potential energy surface in those regions around the TS and the local energy minima. Doherty and Hopfinger[40] made a similar assumption in calculating conformational entropies for single chains of syndiotactic PS. Following this approach,[41] a partition function is defined in terms of a Taylor series expansion about a stationary point on the adiabatic potential energy surface. This expansion is truncated to second order, and the following expression for entropy is obtained from this partition function:

$$S = \frac{R}{2}[n + n \ln \pi R + n \ln T - \ln \mathrm{Det}\, \mathbf{H}] \quad (9)$$

where n is the dimensionality of the potential energy surface, R is the gas constant, and $\mathbf{H}$ is the Hessian of the adiabatic potential energy. Since we are only interested in displacements orthogonal to the IRC at the TS, the negative eigenvalue of the Hessian is omitted when evaluating this expression at the TS.

Calculations were performed on phenyl rings common to two racemic diads in which the backbone dihedral angles ϕ_4, ϕ_1, ϕ_2, and ϕ_5 (see Figure 1) are in the *trans* conformational state. These rings were found in 10 atomistic structures of atactic PS 40-mer glasses that were shown to be amorphous over the length scale of the simulation box and to reproduce the experimental X-ray scattering structure factor for PS glasses. Details about the force field, the method used to generate these glass structures, and the conformational and structural characteristics of the glasses are given elsewhere.[30] Ten phenyl rings, distributed over six different structures, were identified. None of these rings were located closer than four monomer units from the chain ends, and no correlation between position along the chain and rotational mobility was observed. The specific location of each ring is given in Table 1. Reaction paths, energy profiles, and free energy barriers for ring rotation were calculated in each case, and rate constants were estimated using the elementary transition state theory rate expression:[23]

$$k = \frac{k_B T}{h} \exp\left(\frac{-\Delta A}{RT}\right) \quad (10)$$

All calculations were performed on SGI 4D/220 or IBM RISC/6000 workstations using our in-house modification of the CHARMM source code.[42]

Results and Discussion

We summarize briefly our previous results for phenyl ring rotation in a single chain of syndiotactic PS hexamer in the *all-trans* conformation of ϕ_4, ϕ_1, ϕ_2, and ϕ_5 before presenting the results for PS glasses. Reaction paths and energy profiles for ring rotation in the glasses are described in detail for selected cases; complete descriptions of all 10 cases can be found elsewhere.[39]

Ring Rotation in a Single Chain. The ϕ_1, ϕ_2, and ϕ_3 profiles along the IRC are plotted in Figure 2a. As ϕ_3 rotates through 180°, both backbone dihedral angles

Table 2. Thermodynamic Properties, TS Theory Rate Constants, and Characteristic Times for Phenyl Ring Rotation in the PS Glass Structures[a]

	energy barrier (kcal/mol)		entropic contributions (kcal/mol)		free energy barrier (kcal/mol)		rate constant (/s/ring)		characteristic time (s)	
case	ΔE_1	ΔE_2	$T\Delta S_1$	$T\Delta S_2$	ΔA_1	ΔA_2	k_1	k_2	t_1	t_2
I	16.03	17.33	0.042	0.135	15.99	17.20	1.4×10^1	1.9	7.1×10^{-2}	5.4×10^{-1}
II	15.06	14.47	1.060	0.543	14.00	13.93	3.9×10^2	4.5×10^2	2.5×10^{-3}	2.2×10^{-3}
III	8.73	12.56	0.72	0.542	8.01	12.02	9.1×10^1	1.1×10^4	1.1×10^{-7}	9.1×10^{-5}
IV	4.59	5.89	−0.051	0.552	4.64	5.34	2.6×10^9	8.1×10^8	3.8×10^{-10}	1.2×10^{-9}
V	7.31	14.61	0.328	0.137	6.98	14.47	5.1×10^7	1.8×10^2	2.0×10^{-8}	5.6×10^{-3}
VI	28.52	28.10	0.66	0.738	27.86	27.36	3.1×10^{-8}	7.3×10^{-8}	3.2×10^7	1.4×10^7
VII	12.84	12.79	0.955	0.429	11.88	12.36	1.4×10^4	6.2×10^3	7.2×10^{-5}	1.6×10^{-4}
VIII	27.63	31.80	−0.99	−1.296	28.62	33.09	8.8×10^{-9}	4.8×10^{-12}	1.1×10^8	2.1×10^{11}
IX	11.00	8.00	0.579	0.645	10.42	7.36	1.6×10^5	2.7×10^7	6.3×10^{-6}	3.7×10^{-8}
X	10.39	12.15	0.636	−0.164	9.75	12.31	4.9×10^5	6.7×10^3	2.0×10^{-6}	1.5×10^{-4}

[a] Subscripts 1 and 2 denote rotation in different directions from the TS configuration.

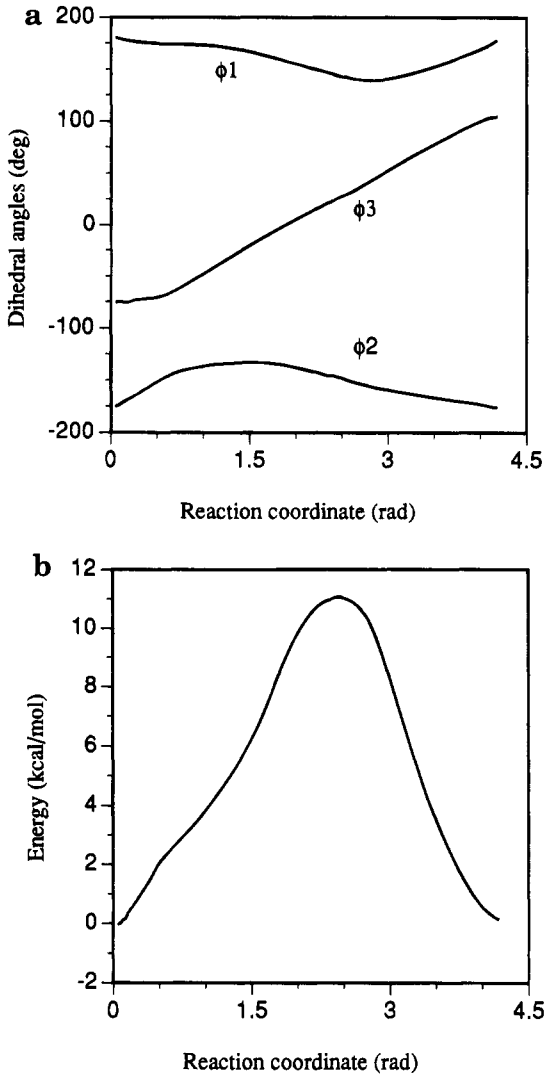

Figure 2. Cooperative phenyl ring rotation in a syndiotactic hexamer of polystyrene in the *tttt* conformation: (a) Torsional angle and (b) energy profiles along the reaction path.

rotate cooperatively by about 40°. This concerted motion occurs to relieve steric interactions between *ortho* hydrogens on the rotating phenyl ring and hydrogens on first and second nearest-neighbor backbone carbon atoms, specifically H23−H16, H23−H17, H27−H22, and H27−H20 in Figure 1. The potential energy profile along the IRC is plotted in Figure 2b. In the TS configuration at ~2.5 rad, the phenyl ring is rotated such that the angle between the plane of the ring and the plane formed by adjacent carbon−carbon bonds on the chain backbone is ~50°, and the *ortho* hydrogens on the ring are in close proximity (~1.95 Å) to hydrogens on the second nearest-neighbor backbone carbon atoms. The potential energy decreases monotonically in both directions from the TS to local energy minima that correspond to the same configuration with the phenyl ring rotated 180°. The energy barrier is approximately 11 kcal/mol.

Ring Rotation in Polystyrene Glasses. The TS configuration in all 10 cases is similar to that obtained for ring rotation in the single chain. The plane of the phenyl ring is rotated by approximately 40−50° from the plane formed by adjacent backbone carbon−carbon bonds, and at least one of the *ortho* hydrogens on the ring is in close proximity to hydrogens on the second nearest-neighbor backbone carbon atoms. These angles and the important hydrogen−hydrogen separations are given in Table 1. In most cases, the important interactions are the H23−H16 and H27−H22 steric interactions, which, in general, have separations less than that obtained for the single chain. Energy barriers, entropic contributions, free energy barriers, and TS theory rate constants for phenyl ring rotation at 300 K are given in Table 2. The characteristic time for ring rotation, defined simply as the reciprocal of the rate constant, is also reported in this table.

In all the cases, the entropic contribution to the free energy barrier for ring rotation amounts to less than 10% of the potential energy barrier. This result is consistent with that of Smith and Boyd,[22] who found the potential energy and free energy profiles for ester side-group reorientation in polyethylene to be essentially identical. Negligible conformational entropies were also assumed by Suter and co-workers[7] in their study of phenyl ring rotation in PS glasses. Our results suggest that their assumption is a reasonable one.

The energy barriers for ring rotation cover a wide range of values corresponding to a distribution of characteristic times that spans 21 decades. For cases VI and VIII, the energy barriers are nearly 30 kcal/mol and the characteristic times are on the order of 10^7−10^{11} s. These rings are effectively immobile on the time scale of the NMR experiments of Spiess[14,15] and Schaefer and co-workers.[16,17] However, a majority of the phenyl rings have characteristic times for rotation on the order of 10^{-8}−10^{-1} s and therefore would be rotationally mobile on the time scale of the NMR experiments. For six cases, the energy barriers are within approximately 4 kcal/mol of the value obtained for ring rotation in the single chain, and for case I, the energy barriers are just above the upper bound of this range. The remaining case IV has unusually low energy barriers of less than

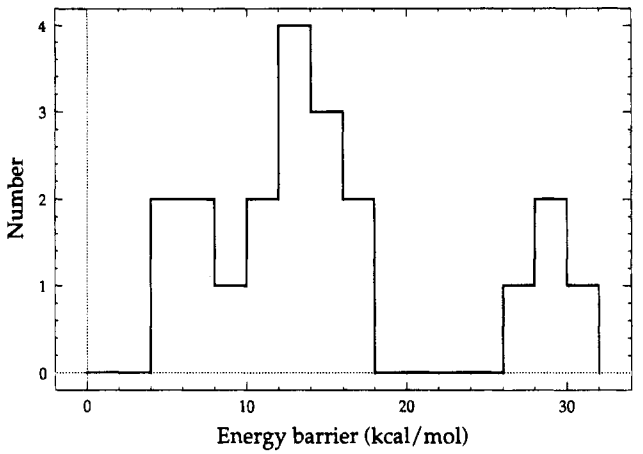

Figure 3. Distribution of energy barriers for ring rotation in PS glass.

Table 3. Change in Ring Dihedral and Reorientational Angles between the TS Configuration and the Minimum-Energy Configurations M1 and M2

	change in ring dihedral angle (deg) between		ring reorientation angle (deg) between	
case	TS and M1	TS and M2	TS and M1	TS and M2
I	77	100	83	95
II	80	72	85	65
III	50	46	49	46
IV	40	34	34	34
V	50	110	51	102
VI	68	104	69	106
VII	85	96	82	99
VIII	81	93	89	86
IX	71	41	72	38
X	65	80	71	75

6 kcal/mol. However, this case corresponds to severely restricted rotation of only 75° (see Table 3).

The distribution of energy barriers is also bimodal, as shown in Figure 3, with no values between approximately 17 and 27 kcal/mol. The distribution below 17 kcal/mol is centered roughly on the energy barrier we obtained for ring rotation in the single chain. Bimodal distributions of NMR rotational correlation times were reported by Spiess[14,15] and by Schaefer and co-workers.[16,17] However, the fraction of rotationally mobile rings found in their work is substantially less than that observed here. This discrepancy may be attributed, at least in part, to the fact that we studied ring rotation for only one local chain conformation, while the NMR correlation times correspond to ring rotation averaged over all conformations.

An analysis of the TS conformations—specifically, the separation between *ortho* hydrogens on the rotating ring and hydrogens on the second nearest-neighbor backbone carbon atoms (see Table 1)—indicates that steric interactions between these hydrogens are more unfavorable in the glass than they are in the single chain. For single chains, these interactions are relieved by a concerted motion of the chain backbone, manifested in the rotation of ϕ_1 and ϕ_2 by approximately 40°. In the glass, however, any such movement of backbone encounters larger resistances due to interchain packing, and, in most cases, ϕ_1 and ϕ_2 rotate by only 20–30°. As an example, consider the torsion angle and potential energy profiles along the IRC shown in Figure 4 for case I. Comparing the torsion angle profiles with those in Figure 2 for the single chain, it is clear that ϕ_2 follows essentially the same trajectory in both cases, while ϕ_1 does not rotate as much in the glass. As a consequence,

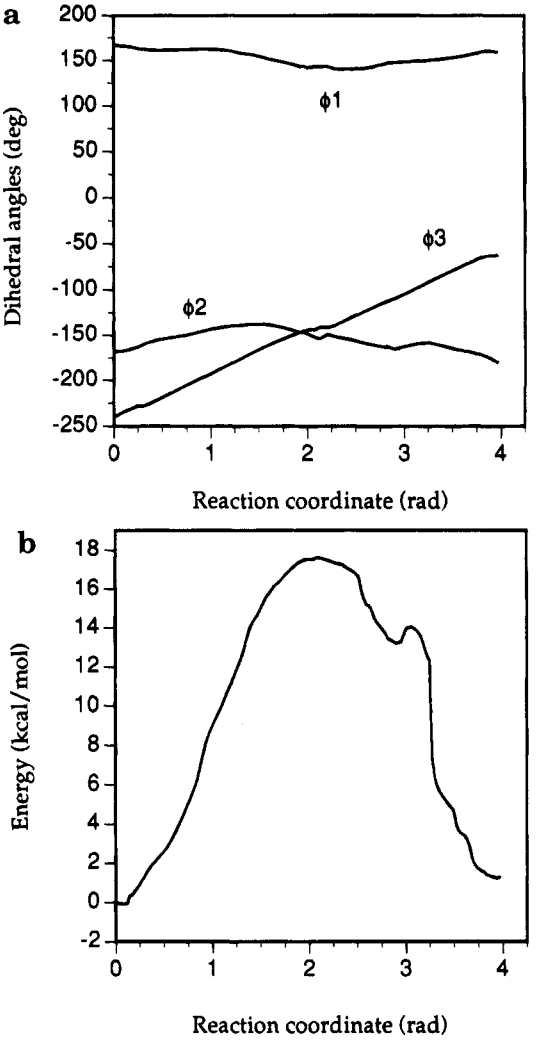

Figure 4. Cooperative rotation in polystyrene glass. Case I: (a) Torsional angle and (b) energy profiles along the reaction path. (The local energy maximum at ~3.1 rad is on the order of the average thermal energy and hence is not a true TS.[43])

the H23–H16 steric interactions, which are relieved by the concerted rotation of ϕ_1 (see Figure 1), are much greater in the glass. The H23–H16 separation in the TS configuration for the glass is 1.85 Å (Table 1), compared to 1.95 Å for the single chain. Thus, higher energy barriers of 16–17 kcal/mol are obtained for ring rotation in the glass, compared to 11 kcal/mol for rotation in the single chain.

These unfavorable steric interactions are also present in those glasses where the potential energy barrier for ring rotation is less than that for the single chain. However, lower energy barriers are obtained in each of these cases because ϕ_3 does not execute a full 180° rotation (see Table 3) and the reaction path is restricted to one in which one or both minimum-energy configurations have energies greater than that for the single chain. In case III, these steric interactions can become so unfavorable that ϕ_3 rotates by less than 100° along the IRC. Torsion angle and potential energy profiles for this case are shown in Figure 5. Restrictive cooperative movement of the chain backbone is evident from the limited rotation of ϕ_1 and, more significantly, from the displacement of ϕ_2, which rotates by ~30° but does not return to its original position. The rotation of ϕ_2 is confined in one direction along the IRC by steric interactions between *ortho* hydrogens on the rotating ring (ring 35 on the chain) and hydrogens on phenyl

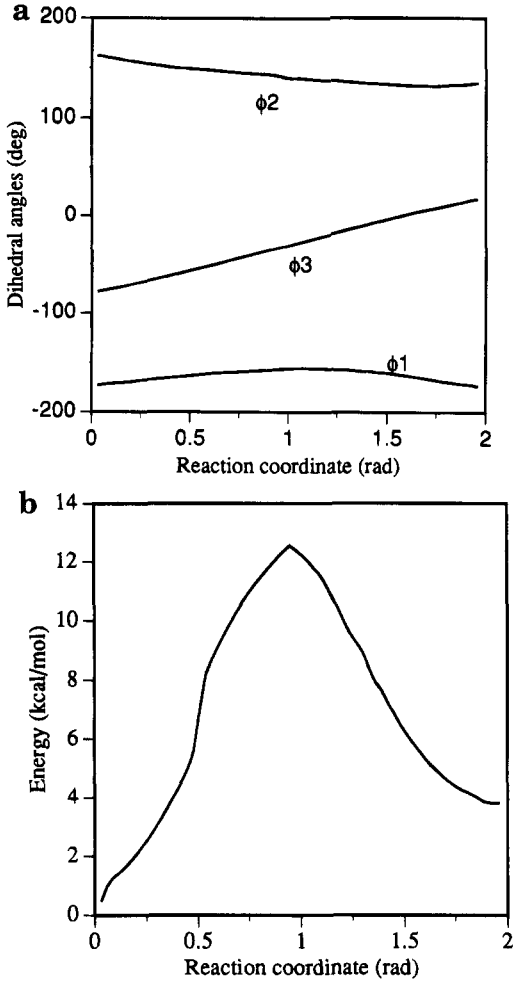

Figure 5. Cooperative rotation in polystyrene glass. Case III: (a) Torsional angle and (b) energy profiles along the reaction path.

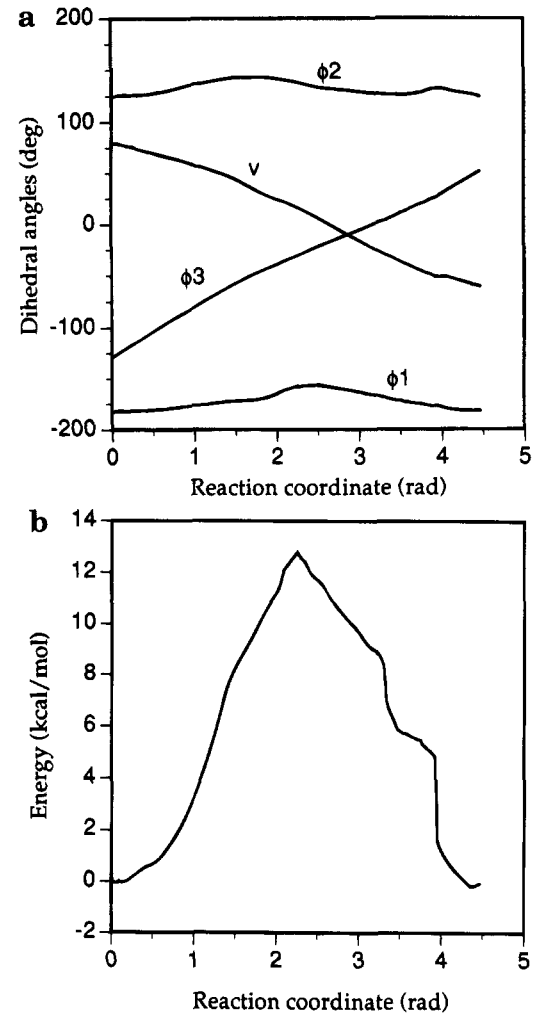

Figure 6. Cooperative phenyl ring rotation in polystyrene glass. Case VII: (a) Torsional angle and (b) energy profiles along the reaction path. v denotes the virtual dihedral angle described in the text.

rings 18 and 21, which cannot be relieved without rearrangements involving a large number of torsional angles. In the absence of such rearrangements, ϕ_3 rotates by only 46° between the TS configuration and the minimum-energy configuration, M2. A relatively low energy barrier of 9 kcal/mol is obtained because M2 is a relatively high-energy configuration. In the other direction, ϕ_2 is not mobile enough to relieve steric interactions between *ortho* hydrogen, H27, and H20 on the first nearest-neighbor backbone carbon atom. This prevents the ring dihedral angle from rotating more than 50° between the TS configuration and the minimum-energy configuration, M1. In this case, however, M1 is a relatively stable configuration, and thus a much larger energy barrier of 13 kcal/mol is obtained.

The cooperative nature of the ring flip transition in all 10 cases was found to arise in response to local intrachain steric interactions between the rotating phenyl ring and the chain backbone. This observation does not imply, however, that nonlocal interactions are unimportant. Indeed, these interactions may be implicated indirectly through interchain packing, which restricts chain backbone mobility in the glasses. Other nonlocal interactions can also play a role. For case VII, initial attempts to locate the TS using ϕ_1, ϕ_2, and ϕ_3 as the mapping coordinates were unsuccessful due to additional steric interactions between the *para* hydrogen on the rotating ring (ring 21) and the *para* hydrogen on ring 30. Thus, the virtual dihedral angle, defined by the atoms C11–C12–C13–H25 on ring 30, was added as a mapping coordinate to account for this interaction. It is not clear which metric correction should be used to determine the SD path in this case. However, in previous work,[29] it was shown that SD paths determined with and without the metric correction were qualitatively the same. Therefore, we did not apply the metric correction to determine SD paths here. The profiles for ϕ_1, ϕ_2, and ϕ_3 and this virtual dihedral angle are shown in Figure 6a, and the potential energy profile is shown in Figure 6b. As ϕ_3 rotates through 180°, ϕ_1 and ϕ_2 show expected displacements of approximately 20–25° and the virtual dihedral angle changes by ~140°. However, the energy barrier is not significantly different from that obtained for ring rotation in the single chain. Evidently the cooperative movement of the second phenyl ring is not energetically important, nor does it alter the intrinsic "local" character of the transition.

For case VI, the nonlocal interactions are more complicated. The IRC determined in the space of ϕ_1, ϕ_2, and ϕ_3 gave a potential energy profile with a large discontinuity of almost 8.5 kcal/mol at ~2.7 rad (Figure 7b,c). The origin of this discontinuity was determined to be physical in nature and not computational (*e.g.*, due to incomplete minimizations in the SD path determination). An examination of displacements of all nonessential torsion angles across the discontinuity revealed substantial changes of approximately 10° in several

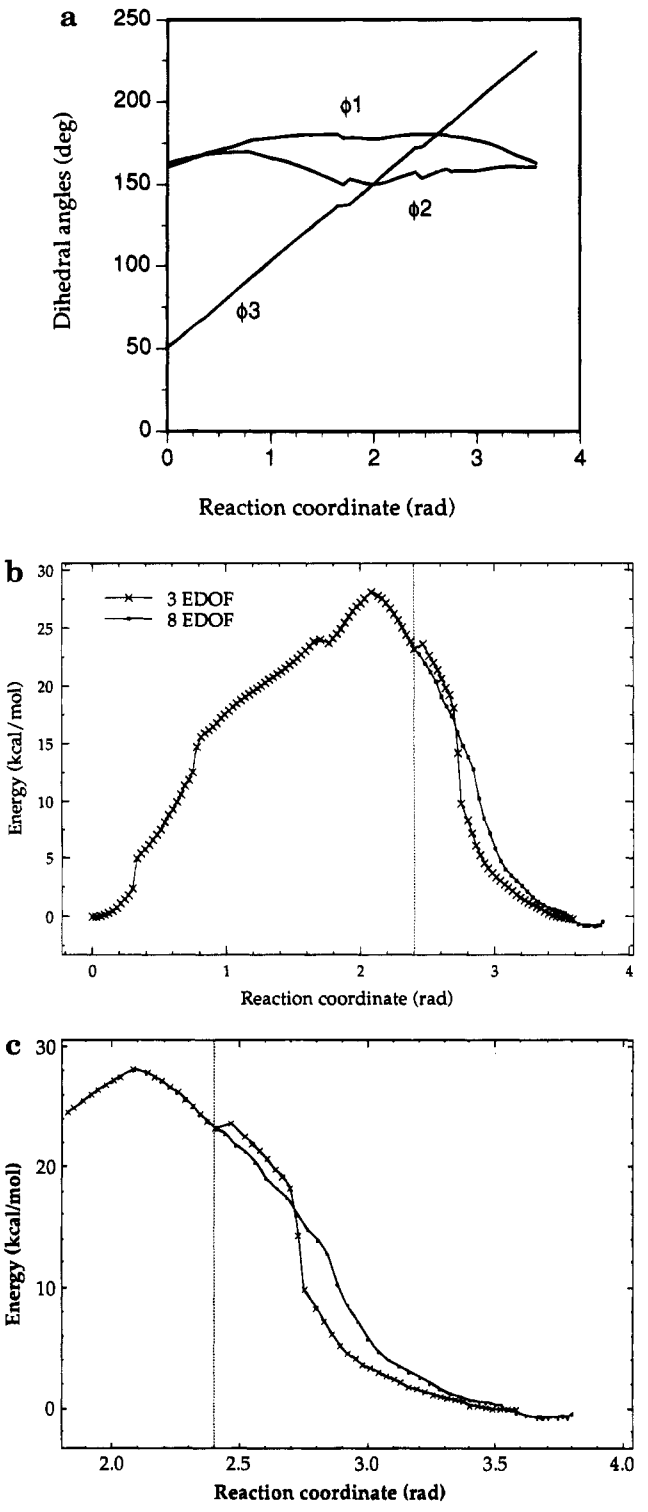

Figure 7. Cooperative phenyl ring rotation in polystyrene glass. Case VI: (a) Torsional angle and (b) energy profiles along the reaction path. A section of b is enlarged as c.

local and nonlocal torsion angles. The local torsion angles were ϕ_4, ϕ_5, and the backbone dihedral angle adjacent to ϕ_5, and the nonlocal torsion angles were ϕ_3 for rings 36 and 40, which are within 5–6 Å of the rotating ring of interest (ring 6).

Reaction path determinations were carried out in which each of the nonlocal torsion angles was added as a fourth mapping coordinate and then with both angles added as two additional mapping coordinates. A large discontinuity of 5–7 kcal/mol was still observed in the potential energy profile in all three cases. Reaction path determinations were also carried out in which ϕ_1, ϕ_2, ϕ_3, and ϕ_5 were considered collectively as essential degrees of freedom along the IRC. This reaction path also failed to eliminate the discontinuity in the potential energy profile. Finally, the reaction path was determined by considering collectively all eight torsion angles: ϕ_1, ϕ_2, ϕ_3, ϕ_4, ϕ_5, the backbone dihedral angle adjacent to ϕ_5, and two virtual dihedral angles accounting for rotation of rings 36 and 40. This 8-dimensional SD path calculation was initiated from the structure at 2.4 rad on the original IRC. The resulting energy profile along the IRC is compared to the original one in parts b and c of Figure 7, where it can be seen that the large discontinuity in potential energy has been eliminated. The angles ϕ_1, ϕ_2, and ϕ_3 have almost identical profiles along the two reaction paths, although differences in ϕ_3 of about 8° were noted in the minimum-energy configurations near 3.6–3.8 rad. The three additional backbone dihedral angles rotate cooperatively by 25°, 30°, and 15° along the IRC. The two minimum-energy configurations were also compared for structural differences by checking relative displacements in the positions of all atoms. The only atoms for which relative displacements were greater than 0.5 Å were those belonging to the rotating phenyl ring, which is a consequence of the ~8° difference in ϕ_3 for the two structures. We conclude, therefore, that the two minimum-energy conformations are essentially the same. It is interesting to note that, although we did not carry out the reaction path determination for the 8-dimensional ring flip transition in the vicinity of the TS, the two potential energy profiles in parts b and c of Figure 7 are not that different away from the discontinuity toward the TS. Therefore, the potential energy barrier may not be greatly influenced by these additional local and nonlocal interactions.

To check whether additional torsion angles should be accounted for explicity in the reaction path determinations, we calculated the following correlation coefficient for each dihedral angle, ϕ_i, from structures stored at regular intervals along the reaction path,

$$c_i = \frac{\sum_j \Delta\phi_{ij}\Delta\phi_{3j}}{\sum_j \Delta\phi_{3j}\Delta\phi_{3j}} \qquad (11)$$

where the sum is carried out over all structures along the reaction path and $\Delta\phi_{ij}$ denotes the difference in values of ϕ_i between the successive structures. A typical value of $\Delta\phi_{3j}$ is 5–10°. If ϕ_i is correlated with ϕ_3, then the absolute value of this coefficient will be close to unity; if the two torsional angles are completely uncorrelated, this coefficient will be zero. We adopt an *ad hoc* measure of the extent of this correlation and consider ϕ_i to be correlated with ϕ_3 if the coefficient has a value greater than 0.2.

In each of the 10 cases studied, it was found that at least one additional, local backbone dihedral angle adjacent to ϕ_1 or ϕ_2 exhibits correlated rotation. In two cases, this cooperative movement was found to extend as far as three or four dihedral angles along the chain backbone. Cooperative movement of phenyl rings adjacent to the ring of interest on the chain was also detected in a few cases, and one or more nonadjacent phenyl rings and their corresponding backbone dihedral angles showed correlated rotation in nine cases. Many of these nonadjacent rings were found to be located near

the phenyl ring of interest, such that the distance between ring centroids was on the order of 4.5–6.0 Å. Hence, their cooperative movement could be anticipated. However, in three cases, the mechanism for this cooperative behavior was not apparent since the phenyl ring was separated from the rotating ring by more than 9 Å. Suter and co-workers also observed nonlocal cooperative behavior for ring rotation in polycarbonate[21] and polystyrene[7] glasses and attributed it to "soft" regions in the glass where flexible chain backbones can readily respond to chain motions even at remote separations.

Conclusions

Our results show that local intrachain interactions, that dominate rotation in single chains, do so in the polymer glass as well. These intrachain interactions involve *ortho* hydrogens on the rotating phenyl ring and hydrogens on the second nearest-neighbor backbone carbon atoms and are relieved by the cooperative motion of the rotating ring and the chain backbone through the rotation of dihedral angles, ϕ_1 and ϕ_2. In the glass, these backbone dihedral angles typically rotate by ~20–30°, which is less than that observed in the single chain (~40°). The lower flexibility of chain backbones in the glass, which is a consequence of interchain packing, leads to higher-energy TS conformations and, hence, higher energy barriers for ring rotation in the glass.

Our approach to defining cooperative ring rotation represents a compromise between the extremes of defining the IRC in the space of Cartesian coordinates for all the atoms in the system and defining it using only one internal coordinate, ϕ_3. Reaction path determinations in the space of Cartesian coordinates of all atoms are computationally demanding due to the large dimensionality of the Hessian, while an approach using only ϕ_3 does not account for the cooperative nature of the motion. Rapold *et al.*[7] calculated energy barriers for phenyl ring rotation in PS glasses using only ϕ_3 and obtained potential energy profiles with multiple jump discontinuities on the order of 25 kcal/mol (see, for example, Figure 12 in ref 7). The energy profiles calculated here on the basis of three essential degrees of freedom do not exhibit these large discontinuities. Only 4 of our 20 SD paths have energy profiles with discontinuities as high as 2–5 kcal/mol. In the one case where a large jump of ~8.5 kcal/mol was observed (Figure 7), it was found that this discontinuity could be eliminated by systematiclly adding five additional mapping coordinates that showed correlated movement with ϕ_1, ϕ_2, and ϕ_3. Thus, we conclude that the discontinuities obtained by Rapold *et al.*[7] can be attributed, at least in part, to their definition of the reaction coordinate in terms of only ϕ_3, which in effect neglects the cooperative nature of the transition. Moreover, we also observed small changes in bond angles during the adiabatic energy minimizations, whereas Rapold *et al.*[7] fixed the bond angles in their calculations. This relaxation is likely to be energetically important and, thus, may also contribute to the large discontinuities in their potential energy profiles.

In comparing their simulation results for phenyl ring rotation in PS glasses with NMR results, Rapold *et al.*[7] calculated ring rotation with respect to a fixed, external frame of reference. Based on the criterion that a flip is observed if the phenyl ring rotates by at least 40–50° from the TS, they estimated that only 3–5% of the rings with energy barriers less than 20 kcal/mol would exhibit such a transition. We likewise compared the change in ϕ_3 with a reorientation angle defined as the angle between the vector normal to the plane of the phenyl ring in the TS and the minimum-energy structures. The results are given in Table 3. In all cases, the difference between ϕ_3 and the reorientation angle is small and, in almost all cases, the reorientation angle is greater than 40–50°. Thus, we would expect a much higher fraction of phenyl rings to execute flips in the NMR experiments. This large discrepancy can be attributed to the fact that we examined ring rotation in only one local chain conformation, whereas Rapold *et al.*[7] investigated all ring environments. In addition, Rapold *et al.*[7] defined the TS as the first local maximum in their energy profile, which seldom gives reorientation angles that are greater than 40–50°.

Locating the TS using the Cerjan–Miller algorithm proved to be cumbersome at times. The progress of the algorithm had to be monitored closely because the search would frequently proceed along a direction in which one of the backbone dihedral angles changed from *trans* to *gauche*. In these instances, where multiple saddle points are readily accessible, the Cerjan–Miller algorithm may not converge to the TS for the transition of interest. This difficulty can be avoided by applying the Czerminski–Elber method in which the system is forced to find a reaction path connecting two specified minimum-energy configurations. It must be pointed out, however, that the Czerminski–Elber method does not guarantee that the TS it locates will be a stationary point with only one negative eigenvalue in the Hessian. This method also requires a large number of grid points along the reaction path in the vicinity of the TS if an accurate location is desired.

Identifying the essential degrees of freedom is a critical step in our methodology and requires some physical intuition. In systems as complicated as amorphous polymers, it is likely that multiple paths exist that connect two minima on the potential energy surface, and different sets of essential degrees of freedom may be required to define the different pathways. We did not perform an exhaustive search for all pathways describing the cooperative rotation because this task would be computationally intractable. Instead, we relied on physical insights obtained from our simulation studies of single polymer chains, where local intrachain interactions were observed to govern the ring flip process. Since these interactions must also be present for ring rotation in the glass, we initiated our reaction path determinations in the glass using the single-chain mapping coordinates as a starting point and extended our calculations to include additional local or nonlocal degrees of freedom when necessary. These additional mapping coordinates were identified by an analysis of the structures and the potential energy profile along the IRC. The ability to carry out a systematic analysis of structures along the reaction path and to apply physical intuition to refine the reaction path are important advantages of this internal coordinate approach to multidimensional reaction path determinations.

References and Notes

(1) Helfand, E.; Wasserman, Z. R.; Weber, T. A. *Macromolecules* **1980**, *13*, 526.
(2) Adolf, D. B.; Ediger, M. D. *Macromolecules* **1992**, *25*, 1074.
(3) Adolf, D. B.; Ediger, M. D. *Macromolecules* **1991**, *24*, 5834.
(4) Takeuchi, H.; Roe, R.-J. *J. Chem. Phys.* **1991**, *94*, 7458.
(5) Boyd, R. H.; Gee, R. H.; Han, J.; Jin, Y. *J. Chem. Phys.* **1994**, *101*, 788.

(6) Tiller, A. R. *Macromolecules* **1992**, *25*, 4605.
(7) Rapold, R. F.; Suter, U. W.; Theodorou, D. N. *Macromol. Theory Simul.* **1994**, *3*, 19.
(8) Khare, R.; Paulaitis, M. E. *Chem. Eng. Sci.* **1994**, *49*, 2867.
(9) Illers, K. H.; Jenckel, E. *J. Polym. Sci.* **1959**, *XLI*, 528.
(10) Baccaredda, M.; Butta, E.; Frosini, V. *Polym. Lett.* **1965**, *3*, 189.
(11) Yano, O.; Wada, Y. *J. Polym. Sci., Polym. Phys. Ed.* **1971**, *9*, 669.
(12) Yano, O.; Wada, Y. *J. Polym. Sci., Polym. Phys. Ed.* **1974**, *12*, 665.
(13) Connor, T. M. *J. Polym. Sci., Polym. Phys. Ed.* **1970**, *8*, 191.
(14) Spiess, H. W. *Colloid Polym. Sci.* **1983**, *261*, 193.
(15) Spiess, H. W. *J. Mol. Struct.* **1983**, *111*, 119.
(16) Schaefer, J.; Sefcik, M. D.; Stejskal, E. O.; McKay, R. A.; Dixon, W. T.; Cais, R. E. *Macromolecules* **1984**, *17*, 1107.
(17) Schaefer, J.; Sefcik, M. D.; Stejskal, E. O.; Mckay, R. A.; Dixon, W. T.; Cais, R. E. *ACS Symp. Ser.* **1984**, *247*, 43.
(18) Tonelli, A. E. *Macromolecules* **1973**, *6*, 682.
(19) Hägele, P. C.; Beck, L. *Macromolecules* **1977**, *10*, 213.
(20) Tanabe, Y. *J. Polym. Sci., Polym. Phys. Ed.* **1985**, *23*, 601.
(21) Hutnik, M.; Argon, A. S.; Suter, U. W. *Macromolecules* **1991**, *24*, 5970.
(22) Smith, G. D.; Boyd, R. H. *Macromolecules* **1992**, *25*, 1326.
(23) Glasstone, S.; Laidler, K. J.; Eyring, H. *The Theory of Rate Processes*; McGraw Hill: New York, 1941.
(24) Keck, J. C. *Discuss. Faraday Soc.* **1962**, *33*, 173.
(25) Anderson, J. B. *J. Chem. Phys.* **1973**, *58*, 4684.
(26) Bennett, C. H. In *Algorithms for Chemical Computations*; Christofferson, R. E., Ed.; American Chemical Society: Washington, DC, 1977.
(27) Berne, B. J. In *Multiple Time Scales*; Brackbill, J. U., Cohen, B. I., Eds.; Academic Press: New York, 1985.
(28) Northrup, S. H.; Pear, M. R.; Lee, C.-Y.; McCammon, J. A.; Karplus, M. *Proc. Natl. Acad. Sci. U.S.A.* **1982**, *79*, 4035.
(29) Lazaridis, T.; Paulaitis, M. E. *J. Am. Chem. Soc.* **1994**, *116*, 1546.
(30) Khare, R.; Paulaitis, M. E.; Lustig, S. R. *Macromolecules* **1993**, *26*, 7203.
(31) Fukui, K. *Acc. Chem. Res.* **1981**, *14*, 363.
(32) Elber, R.; Karplus, M. *Chem. Phys. Lett.* **1987**, *139*, 375.
(33) Ulitsky, A.; Elber, R. *J. Chem. Phys.* **1990**, *92*, 1510.
(34) Czerminski, R.; Elber, R. *J. Chem. Phys.* **1990**, *92*, 5580.
(35) Pratt, L. R. *J. Chem. Phys.* **1986**, *85*, 5045.
(36) Gillilan, R. E.; Wilson, K. R. *J. Chem. Phys.* **1992**, *97*, 1757.
(37) Cerjan, C. J.; Miller, W. H. *J. Chem. Phys.* **1981**, *75*, 2800.
(38) Lazaridis, T.; Tobias, D. J.; Brooks, C. L., III; Paulaitis, M. E. *J. Chem. Phys.* **1991**, *95*, 7612.
(39) Khare, R. S. Ph.D. Thesis, University of Delaware, Newark, DE, 1994.
(40) Doherty, D. C.; Hopfinger, A. J. *Comput. Polym. Sci.* **1991**, *1*, 107.
(41) Hopfinger, A. J. *Conformational Properties of Macromolecules*; Academic: New York, 1973.
(42) Brooks, B. R.; Bruccoleri, R. E.; Olafson, B. D.; States, D. J.; Swaminathan, S.; Karplus, M. *J. Comput. Chem.* **1983**, *4*, 187.
(43) Chandler, D. *J. Chem. Phys.* **1978**, *68*, 2959.

MA946255C